



Norwegian University of
Science and Technology

Simulation of a booster pump and a reversible pump turbine in series

John Valstad

Hydropower Development

Submission date: June 2018

Supervisor: Pål Tore Selbo Storli, EPT

Norwegian University of Science and Technology
Department of Energy and Process Engineering

EPT-M-2018-103

MASTER THESIS

for

Student John Valstad

Spring 2018

Simulation of a booster pump and a reversible pump turbine in series

Simulering av en boosterpumpe og en reversibel pumpeturbin i serie

Background

Norway has 50% of the European hydro reservoir energy storage, and many of these sites are highly suitable for retrofitting of pump-storage capabilities. However, this is very expensive using current technologies, and a new concept has been proposed to reduce the cost of installing pumping capacity. This concept introduces a low-pressure booster pump close to the inlet of a Reversible Pump Turbine (RPT, acting as a pump in pumping mode). The combined operation of these two units must be investigated to find the combined performance, and to investigate the operating stability.

Objective: The work will seek to map the performance for both pumping and generating mode of operation of the combination of a booster pump and an RPT.

The following tasks are to be considered:

1. Literature study on the operation, both dynamic and steady state, for the combination of a booster pump and an RPT
2. Develop a simulation tool for dynamic simulation of the operation of this combination
3. Map the performance of this combination in both pump- and turbine mode of operation.
4. If the student goes to Nepal for an excursion, earlier and further work will be presented as a publication and presented at the conference; 8th International symposium on Current Research in Hydraulic Turbines (CRHT-VIII) at Kathmandu University in March 2018

-- ” --

Within 14 days of receiving the written text on the master thesis, the candidate shall submit a research plan for his project to the department.

When the thesis is evaluated, emphasis is put on processing of the results, and that they are presented in tabular and/or graphic form in a clear manner, and that they are analyzed carefully.

The thesis should be formulated as a research report with summary both in English and Norwegian, conclusion, literature references, table of contents etc. During the preparation of the text, the candidate should make an effort to produce a well-structured and easily readable report. In order to ease the evaluation of the thesis, it is important that the cross-references are correct. In the making of the report, strong emphasis should be placed on both a thorough discussion of the results and an orderly presentation.

The candidate is requested to initiate and keep close contact with his/her academic supervisor(s) throughout the working period. The candidate must follow the rules and regulations of NTNU as well as passive directions given by the Department of Energy and Process Engineering.

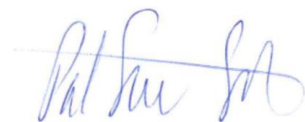
Risk assessment of the candidate's work shall be carried out according to the department's procedures. The risk assessment must be documented and included as part of the final report. Events related to the candidate's work adversely affecting the health, safety or security, must be documented and included as part of the final report. If the documentation on risk assessment represents a large number of pages, the full version is to be submitted electronically to the supervisor and an excerpt is included in the report.

Pursuant to "Regulations concerning the supplementary provisions to the technology study program/Master of Science" at NTNU §20, the Department reserves the permission to utilize all the results and data for teaching and research purposes as well as in future publications.

The final report is to be submitted digitally in DAIM. An executive summary of the thesis including title, student's name, supervisor's name, year, department name, and NTNU's logo and name, shall be submitted to the department as a separate pdf file. Based on an agreement with the supervisor, the final report and other material and documents may be given to the supervisor in digital format.

- Work to be done in lab (Water power lab, Fluids engineering lab, Thermal engineering lab)
- Field work

Department of Energy and Process Engineering, 15. January 2018



Pål-Tore Storli
Academic Supervisor

Co-supervisor: Helene Dagsvik, Magni Fjørtoft Svarstad

Abstract

When considering whether to install a reversible pump-turbine instead of a new Francis turbine in a hydropower plant, the economic aspect is a key factor. The expensive process of submerging the runner, which is needed to avoid cavitation during pump-mode, is essential when calculating whether a reversible pump-turbine is profitable. In this thesis, the possibility of sidestepping the submergence of the runner by installing a booster pump in the forefront of the reversible pump-turbine is investigated.

Results in this thesis are from 1D simulations using the method of characteristics to describe the fluid flow, with the pump performance of an axial flow pump and a reversible pump-turbine modelled by both Suter characteristic curves and dynamic pump models. Additionally, an investigation of how the two pumps operate when implemented in an existing hydropower plant, as a replacement for the Francis turbine in Roskrepp hydropower plant was simulated. Results from the implementation of Suter characteristics curves showed a steady cooperation of the two pumps. Furthermore; positive conclusions can be taken from the simulations of dynamic pump models implemented in Roskrepp which resulted in a steady combined operation able to adapt to forced alterations to the boundary conditions. A start-up operation of the two pumps was similarly simulated in Roskrepp, reaching steady state conditions without significant complications after an initial period of start-up fluctuations. Positive simulation results for the cooperation between a booster pump and a reversible pump-turbine provides an optimistic outlook on the idea.

Sammendrag

Økonomisk lønnsomhet ved installasjon av en reversibel pumpeturbin kontra en ny Francis turbin i eksisterende kraftverk er avhengig av hvor stort inngrep som kreves ved innstallasjon. Ofte må løpehjulet dykkes for å unngå kavitasjon i pumpemodus. Å senke løpehjulet er et kostbart inngrep, som motarbeider profitten av en reversibel pumpeturbin. I denne masteroppgaven vil muligheten for å unngå dykking av vannkraftstasjonen ved å installere en aksiell pumpe i serie med den reversible pumpeturbinen undersøkes. Ved å introdusere en "booster"-pumpe i forkant av sugerøret vil risikoen for kavitasjon reduseres ved å heve trykket ved innløpet til pumpeturbinen.

Resultatene baserer seg på 1D simuleringer ved bruk av karakteristikkmetoden til å implementere vannveien, med både Suter-kurver og dynamiske pumpemodeller brukt til å representere pumpenes drifts-oppførsel. En reversibel pumpeturbin og en "booster"-pumpe blir videre implementert ved bruk av dynamiske pumpemodeller og undersøkt som en mulig erstatning for dagens Francisturbin i Roskrepp kraftverk. Resultatene fra simuleringen ved bruk av Suter-kurver viser et stabilt samarbeid mellom de to pumpene. Videre resulterte simuleringer av en reversibel pumpeturbin og en "booster"-pumpe i Roskrepp kraftverk et stabilt system, kapabelt til å hurtig innrette seg mot påtvungne endringer av grensebetingelsene. En simulering av pumpenes oppstartsfase i Roskrepp kraftverk ble også utført, der stabile driftsforhold ble funnet uten større vanskeligheter etter en startperiode med noe svingninger. Positive simuleringsresultater funnet for samkjøring av en "booster"-pumpe og en reversibel pumpeturbin gir grunn til optimisme for idéen.

Preface

This master thesis is written at the Water Power laboratory at NTNU, for the Department of Energy and Process engineering, during the spring of 2018. The purpose of this master thesis was to continue the work done in the project thesis, investigating the possibility of introducing a booster pump in the forefront of a reversible pump-turbine.

I would like to thank my supervisor Pål-Tore Storli for always being available, answering questions and welcoming discussions. I also want to thank all my fellow students at the Water Power laboratory for collectively creating a good working environment.

Trondheim, June 2018

John Valstad

Contents

Abstract	i
Sammendrag	iii
Preface	v
Table of Contents	viii
List of Tables	ix
List of Figures	xi
Nomenclature	xvi
1 Introduction	1
1.1 Roskrepp hydropower plant	2
1.2 Previous work	2
2 Theory	3
2.1 Cavitation in turbomachinery	3
2.2 Axial flow pump	4
2.3 Reversible pump-turbine	5
2.3.1 Design of reversible pump-turbine	6
2.4 Method of characteristics	7
2.4.1 Boundary conditions	9
2.5 Suter characteristic curves	10
2.6 Dynamic model for a reversible pump-turbine	12

2.7 Valve	16
3 Method	19
3.1 Transient model using Suter characteristic curves	19
3.2 Transient model using dynamic pump models	21
4 Results and discussions	23
4.1 Transient model using Suter characteristic curves	23
4.2 Cooperation using dynamic pump models	26
4.3 Dynamic pump models implemented for Roskrepp	28
4.3.1 Continuous change in boundary conditions	30
4.3.2 Pump start-up in Roskrepp	31
4.4 General discussions about the simulation results	32
5 Conclusion	35
6 Further work	37
Bibliography	39
Appendix	41
6.1 Appendix A - Design reversible pump turbine	41
6.2 Appendix B - Matlab script Roskrepp waterway with RPT and booster pump - continuous periodic reservoir heights	43
6.3 Appendix C - Matlab script function to iterate new flow rate and rotational speed RPT	59
6.4 Appendix D - Matlab script finding RPT dimensions	60

List of Tables

4.1	Values for the reversible pump-turbine	26
4.2	Values for the booster pump	26

List of Figures

2.1	Head-flow characteristics for a typical axial flow pump[9]	5
2.2	Head characteristic curve for a pump-turbine in pumping mode[3]	6
2.3	Graphical visualization of the method of characteristics []	9
2.4	Velocity triangles at inlet and outlet of a reversible pump-turbine[8]	13
3.1	Pipe system used to implement the Suter characteristic curves	20
3.2	Simplified version of the Roskrepp pipe system in which the reversible pump-turbine and the booster pump were implemented	21
4.1	Change in flow rate over time	24
4.2	Head from the pumps, frictional loss in the system and difference in height between the reservoirs over time	24
4.3	Change in flow rate through the pipes	25
4.4	Pump height, flow rate and rotational speed changing with time	27
4.5	Piezometric head along the pipeline	27
4.6	Continuous periodic change in upstream reservoir height	28
4.7	Nominal values over time	29
4.8	Flow rate in different points in the pipeline over time	29
4.9	Nominal values over time with periodic change	30
4.10	Nominal values over time when forces alterations to both reservoir heights	31
4.11	Change in flow rates during start-up	32
4.12	Change in flow rate over the valve during start-up	32

Nomenclature

Acronyms

<i>b.hp</i>	Brake horse power	$\text{kgm}^2\text{s}^{-3}$
<i>BEP</i>	Best efficiency point	-
<i>MOC</i>	Method of characteristics	-
<i>RPT</i>	Reversible pump turbine	-
<i>SCC</i>	Suter characteristic curves	-
<i>tdh</i>	Total dynamic head	m

Greek Symbols

α	Ratio of used vs rated rotational speed	-
α_1	Inlet guide blade angle	$^\circ$
α_2	Outlet guide blade angle	$^\circ$
β	Ratio of used vs rated torque	-
β_1	Inlet vane angle	$^\circ$
β_2	Outlet vane angle	$^\circ$
η	Efficiency	-
κ	Opening degree of the turbine	-
ν	Ratio of used vs rated flow rate	-

ω	Rotational speed	s^{-1}
ρ	Density	kgm^{-3}
τ	Valve degree of opening	-

Roman Symbols

Δt	Time step	s
Δx	Length increment	m
A	Pipe cross-sectional area	m^2
a	Wave propagation speed	ms^{-1}
B	Constant used in MOC	sm^{-2}
c	Ratio of rated flow rates for the pumps	-
C^+	Characteristic equation MOC	-
C^-	Characteristic equation MOC	-
c_1	Inlet absolute velocity	ms^{-1}
c_2	Outlet absolute velocity	ms^{-1}
C_M	Characteristic constant MOC	m
C_P	Characteristic constant MOC	m
C_{311}	Constant for pump 1 used for SCC	-
C_{312}	Constant for pump 2 used for SCC	-
C_d	Discharge coefficient valve	-
c_{m1}	Inlet meridional velocity	ms^{-1}
c_{m2}	Outlet meridional velocity	ms^{-1}
c_{u1}	Inlet peripheral component of the absolute velocity	ms^{-1}

c_{u2}	Outlet peripheral component of the absolute velocity	ms^{-1}
D	Pipe diameter	m
f	Friction factor	-
g	Gravity	ms^{-2}
H	Head	m
h	Ratio of delivered vs rated head	-
I_p	Polar moment of inertia generator	kgm^2
I_h	Hydraulic inertia turbine	m^{-1}
L	Pipe length	m
$NPSH_A$	Net positive suction head available	m
$NPSH_R$	Net positive suction head required	m
P	Pressure	Pa
Q	Flow rate	m^3s^{-1}
R	Constant used in MOC	s^2m^{-5}
u_1	Inlet peripheral velocity	ms^{-1}
u_2	Outlet peripheral velocity	ms^{-1}
V	Velocity	ms^{-1}
v_1	Inlet relative velocity	ms^{-1}
v_2	Outlet relative velocity	ms^{-1}

Subscripts

0	Steady-state	-
01	Referring to pump 1 at previous time step	-

02	Referring to pump 2 at previous time step	-
1	Starting point segment	-
2	Ending point segment	-
α_{P_1}	Derivative with respect to α_{P_1}	-
α_{P_2}	Derivative with respect to α_{P_2}	-
ν	Derivative with respect to ν	-
f	Friction loss	-
i	Present point in space	-
$i + 1$	Point after present point in space and time	-
$i - 1$	Point before present point in space and time	-
LOW	Lower reservoir	-
P	Present point in space and time	-
R	Rated quantity	-
RES	Upper reservoir	-
t	Turbine	-
ν	Valve	-

1. *Introduction*

Along with the commitment towards increasing use of renewable energy among the worlds leading countries, hydropower is growing as a vital, stable energy source. Hydropower can, by storing water in high-altitude reservoirs, provide a stable energy supply in combination with the fluctuating production in wind, solar and other renewable energy sources. Introducing reversible pump-turbines is beneficial for acquiring a balance in the energy market, both regarding regulation purposes and for the opportunity to store water in reservoirs leaving the marked capable of handling energy droughts. Another aspect is the possible economic benefit while operating a reversible pump-turbine, exploiting the variable electricity prize. Using energy to pump water to the upper reservoir at low cost, storing the water until the price returns to a profitable level, at which point the turbine starts generating power again.

Traditionally, when replacing a turbine with a reversible pump-turbine, an expensive process where the runner is submerged several meters in order to avoid the risk of cavitation is needed. In many situations, this process causes a reversible pump-turbine to be non-profitable when compared to installing a new Francis turbine. In this master thesis, the possibility of bypassing this high-cost operation is explored. By introducing a booster pump in the forefront of the reversible pump-turbine the need to submerge the runner will be eliminated, thus increasing the profitability. Including a booster pump reduces the risk of cavitation in the runner by lifting the inlet pressure of the reversible pump-turbine. Studies of cooperation between the pumps are done using both Suter characteristic curves and dynamic pump models.

1.1 Roskrepp hydropower plant

Located in Oeatvatn, Vest-Agder the Roskrepp hydropower plant is one of seven Sira-Kvina hydropower plants. With a rated head at $90m$ and a discharge of $70m^3/s$, a single Francis turbine has been working since 1979. In recent time the option of replacing the Francis turbine with a reversible pump-turbine has been discussed.

1.2 Previous work

Numerous theses on transient studies of hydropower plants have been written. No thesis has, however, been focused on the possibility of introducing a booster pump in the forefront of a reversible pump-turbine.

To model the waterway of the hydropower plant the method of characteristics is utilized as outlined in "Fluid Transients"[11] along with inspiration from the master of Anna Holm Aftret[4], which also implemented a waterway using the method of characteristics. Modelling the dynamic pump models follows the method of Torbjørn K.Nielsen[8] and Pål-Tore Storli[10].

2. Theory

When replacing a turbine with a reversible pump-turbine multiple variables need to be considered. In this thesis, installing a booster pump to avoid cavitation in the pump-turbine runner is the main objective. Why the idea of introducing a booster-pump can be beneficial is shown by looking at what causes cavitation.

2.1 Cavitation in turbomachinery

Cavitation occurs when the local pressure falls below the vapour pressure, causing the fluid to vaporize, creating vacuum bubbles. The cavitation bubbles appear only to collapse almost instantly damaging the turbomachinery. A limit to when cavitation will occur is found from the Bernoulli equation. The limit is the difference between the pump inlet pressure head and the vapour pressure head. It is called the net positive suction head, or *NPSH*[2].

$$NPSH = \left(\frac{P}{\rho g} + \frac{V^2}{2g} \right)_{pump\ inlet} - \frac{P_{VP}}{\rho g} \quad (2.1)$$

Using piezometric head values, the net positive suction head is expressed as:

$$NPSH = H_A - H_{VP} \pm H_S - H_L + H_V \quad (2.2)$$

Where H_L is the pressure head from the losses, H_V the velocity head at the suction port, H_A the atmospheric pressure head and H_{VP} the vapour pressure head. H_S is the height difference between the center of the pump runner and the downstream water level, which is positive when the pump is below the downstream water level[2]. In or-

der to avoid cavitation in the turbomachinery, the available $NPSH$ needs to exceed the required $NPSH$.

$$NPSH_A > NPSH_R \quad (2.3)$$

While the available $NPSH$ for a pump is given by equations 2.1 and 2.2 will the required $NPSH$ be provided by the pump manufacturer after experimental research[2]. To pinpoint why accessing cavitation is essential when installing a reversible pump-turbine, the losses in the system have to be addressed. While operating the hydropower plant in turbine mode, the friction head loss contributes positively to the available $NPSH$. In pumping mode will, however, the friction loss reduce the available $NPSH$. Traditionally, in order to avoid cavitation when installing a reversible pump-turbine, increasing H_S by submerging the runner is the solution. As an alternative solution, introducing a booster pump to increase the pump-turbine inlet pressure reduces the risk for cavitation by increasing the available $NPSH$.

2.2 Axial flow pump

Introducing a booster pump in the forefront of the reversible pump-turbine requires minimal disturbance of the flow pattern to ensure healthy working conditions for the reversible pump-turbine. The idea is to introduce a rim-driven thruster as the booster pump. The rim-driven thruster utilizes a shaftless ring propulsor with a magnetic rotor embedded in the rim, and the motor stator mounted in the tunnel[1]. By operating in an axial direction, the rim-driven thruster will disturb the direction of the flow minimally. Due to lack of known characteristics for a rim-driven thruster and the similarity to an axial flow pump, is the theoretic background for the rim-driven thruster based on axial flow pumps.

Axial flow pumps, unlike a reversible pump-turbine, do not utilize centrifugal forces. Instead, the rotor blades are formed like airfoils to produce lift and change the momentum in the fluid. The performance of an axial pump depends on the same variables as for an airfoil; the blade twist angle, the blade pitch angle, the blade chord length and the number of blades on the rotor[2]. An axial flow pump will as seen in figure 2.1 provide a broad range of operating flow rates as the head delivered decreases slowly with

increasing flow. Compared to a centrifugal pump, an axial flow pump will typically contribute with less head, but with a larger flow rate[9]. To achieve minimal impact on the

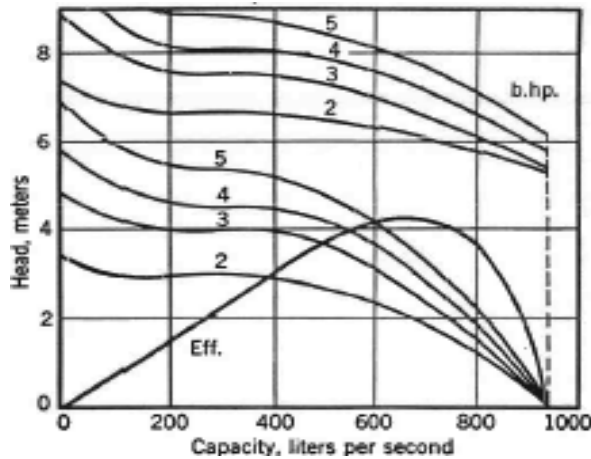


Figure 2.1: Head-flow characteristics for a typical axial flow pump[9]

flow a two-stage counter rotating pump would be beneficial. With two rotors in series, rotating in opposite directions, the swirl inflicted on the fluid from the pumps will cancel each other. Installing two rim-driven thrusters in series would be a similar physical situation, except for the boundary effects from the shaft and blade tips. By itself, the operation of an axial flow pump is stable, as the head delivered continuously decrease with increasing flow rate. This will also be true for a two-stage counter-rotating axial pump[5].

2.3 Reversible pump-turbine

Reversible pump-turbines are a combination of a Francis turbine and a centrifugal pump. Designed to operate as a turbine in one rotational direction, and as a pump in the other rotational direction. Compared to a Francis turbine a pump-turbine will, naturally, have geometrical differences in the runner. As a result of that, the characteristic curve will deviate both from a typical centrifugal pump in pump-mode and from a typical Francis turbine in turbine mode.

In figure 2.2 the pump characteristic for a high head reversible pump-turbine in pump-mode shows an unstable region operating at low flow rates. The gradient of the

characteristic curve reveals an instability in the pump operation. If the slope turns positive it indicates that some of the energy transmitted to the fluid does not contribute to the head delivered. This energy dissipates and creates unsteady flow patterns, thus giving an instability criterion[3].

$$\frac{\partial H}{\partial Q} > 0 \quad (2.4)$$

Exploring the possibility of running a booster pump and a reversible pump-turbine in series requires an assumption that the combined characteristic curve merely is adding one to the other, which leaves a combined pump characteristic that still contains an unstable region for low flow rates.

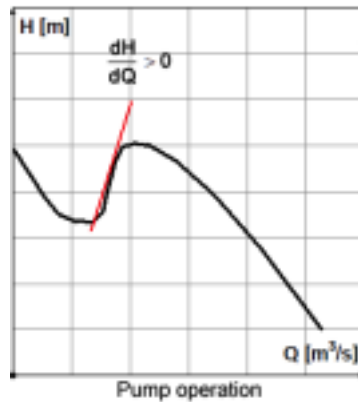


Figure 2.2: Head characteristic curve for a pump-turbine in pumping mode[3]

2.3.1 Design of reversible pump-turbine

Roskrepp hydropower plant has a Francis turbine which operates at given rated values for flow rate and rotational speed. When installing a reversible pump-turbine as a replacement, it is natural to use the same dimensions as the current Francis turbine. Given the rotational speed, the flow rate and the generator size, achieving a fitting reversible pump-turbine can be accomplished by following the same procedure as to designing a Francis turbine. The only exception is setting a reduced inlet peripheral velocity, u_1 , slightly higher than for a Francis turbine[6]. Forcing the pump discharge diameter to be larger than the existing Francis turbine inlet diameter. The design process is described more detailed in Appendix A.

2.4 Method of characteristics

Fluid flow can be either steady-state or transient. To simulate transient flow through a hydropower plant requires a set of initial conditions. It is common to use steady-state flow properties as initial conditions, which is found from the energy equation[2].

$$H_1 + \frac{V_1^2}{2g} + H_p = H_2 + \frac{V_2^2}{2g} + H_t + H_f \quad (2.5)$$

Where H is the pressure head, H_p and H_t the head given from pumps and turbines respectively, and V the velocity. H_f is the friction head loss given by the Darcy-Weisbach equation[2].

$$H_f = \frac{fLQ^2}{2gDA^2} \quad (2.6)$$

However, with the transient study, the operational point changes, leaving the fluid properties to change as well. Therefore, transient fluid flow is governed by the unsteady equation of motion and continuity. Simplified versions of the equations are used when computing transient effects[11].

$$L_1 = g \frac{\partial H}{\partial x} + \frac{\partial V}{\partial t} + \frac{f}{2g} V |V| = 0 \quad (2.7)$$

$$L_2 = \frac{\partial H}{\partial t} + \frac{a^2}{g} \frac{\partial V}{\partial x} = 0 \quad (2.8)$$

By introducing a linear multiplier $\lambda = \pm g/a$, where a is the wave propagation speed, $a = \partial x/\partial t$, and by allowing x to be a function of time, the equations 2.7 and 2.8 can be combined into a ordinary differential equation. In fluid flow the wave propagation speed, a , is approximately 1200m/s[7].

$$\lambda \frac{\partial H}{\partial t} + \frac{\partial V}{\partial t} + \frac{fV|V|}{2D} = 0 \quad (2.9)$$

By substituting both the positive and negative value of λ into 2.9, the method of characteristics transform equations 2.9 into to two pairs of total differential equations; the

C^+ and C^- equations.

$$C^+ = \begin{cases} \frac{\partial x}{\partial t} = a \\ \frac{g}{a} \frac{\partial H}{\partial t} + \frac{\partial V}{\partial t} + \frac{fV|V|}{2D} = 0 \end{cases} \quad (2.10)$$

$$C^- = \begin{cases} \frac{\partial x}{\partial t} = -a \\ -\frac{g}{a} \frac{\partial H}{\partial t} + \frac{\partial V}{\partial t} + \frac{fV|V|}{2D} = 0 \end{cases} \quad (2.11)$$

With the linear multiplier λ implemented into the partial differential equations 2.7 and 2.8, two ordinary differential equations are formed. These ODE's can be solved numerically by a finite difference approximation[11].

$$C^+ : H_{Pi} = C_P - BQ_{Pi} \quad (2.12)$$

$$C^- : H_{Pi} = C_M + BQ_{Pi} \quad (2.13)$$

Where

$$C_P = H_{i-1} - BQ_{i-1} + RQ_{i-1} | Q_{i-1} | \quad (2.14)$$

$$C_M = H_{i+1} + BQ_{i+1} - RQ_{i+1} | Q_{i+1} | \quad (2.15)$$

and

$$R = \frac{f\Delta x}{2gDA^2} \quad B = \frac{a}{gA} \quad (2.16)$$

Where subscripts $i-1$ and $i+1$ refer to points in front of and behind the present point in space at the previous time step, as seen graphically in figure 2.3. When simulating transient flow through pipes, the pipes in the waterway are divided into small increments, Δx . This sets the time step combined with the wave propagation speed a .

$$\Delta t = \frac{\Delta x}{a} \quad (2.17)$$

Finally, with equation 2.14 and 2.15, both the pressure and the flow rate in point P can be calculated[11].

$$H_{Pi} = \frac{C_P + C_M}{2} \quad (2.18)$$

$$Q_{Pi} = \frac{C_P - C_M}{2B} \quad (2.19)$$

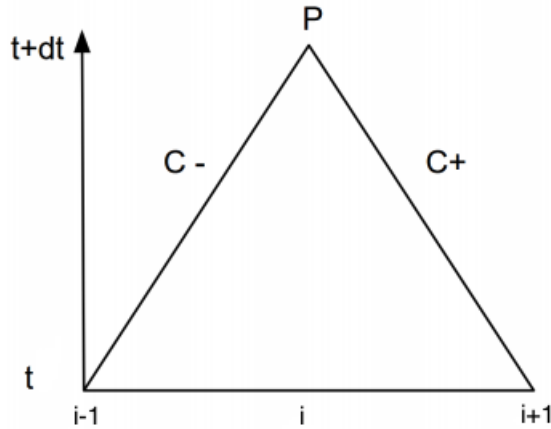


Figure 2.3: Graphical visualization of the method of characteristics []

2.4.1 Boundary conditions

Implementation of a transient model needs set boundary conditions. For a simple system pumping water from a lower to a higher reservoir four boundary conditions are required; at the pipe inlet, the pump inlet, the pump discharge and the pipe outlet. Having large reservoirs leaving the surface height unaffected by the pipe flow, the boundary conditions at the pipe inlet and the pipe outlet are equal to the pressure at the reservoir surface height[11].

$$\text{Inlet: } H_{P_i} = H_{LOW} \quad \text{Outlet: } H_{P_i} = H_{RES} \quad (2.20)$$

With the flow rate boundary conditions given by equations 2.10 and 2.11:

$$\text{Inlet: } Q_{P_i} = \frac{H_{P_i} - C_M}{B} \quad \text{Outlet: } Q_{P_i} = \frac{C_P - H_{P_i}}{B} \quad (2.21)$$

Where C_P and C_M are given by equations 2.14 and 2.15. The boundary conditions at the pump inlet and discharge are found from an iterative process using Suter characteristic curves. When new values for flow rate through the pumps are obtained, the boundary conditions can be updated. Combining C_P , C_M and the new flow rate provide boundary

conditions at the pump inlet and discharge[11].

$$Q_{P_i, \text{pumpinlet}} = Q_{\text{iterated}} \quad H_{P_i, \text{pumpinlet}} = C_P - BQ_{P_i, \text{pumpinlet}} \quad (2.22)$$

And at the pump discharge:

$$Q_{P_i} = Q_{P_i, \text{pumpinlet}} \quad H_{P_i} = t dh_{P_1} + t dh_{P_2} + H_{P_i, \text{pumpinlet}} \quad (2.23)$$

Where $t dh_{P_1}$ and $t dh_{P_2}$ are the head contributed from the two pumps at the iterated flow rate.

By adding more detail to the pipe system, added boundary conditions are needed. Introducing pipes with different cross-sectional areas to the pipe system, requires two extra boundary conditions at the junction. Continuity demands that the flow rate is equal at both sides and by assuming no distance between the end nodes in the each of the attaching pipes, the piezometric head is also equal at both points.

$$Q_1 = Q_2 \quad H_1 = H_2 \quad (2.24)$$

With subscripts 1 and 2 pointing to the nodes before and after the junction. These conditions combined with equations 2.21 are used to find the flow rate and pressure head at both sides of the junction.

$$Q_1 = Q_2 = \frac{C_{P1} - C_{M2}}{B_1 + B_2} \quad H_1 = H_2 = C_{M2} + B_2 Q_2 \quad (2.25)$$

2.5 Suter characteristic curves

Simulations of the combined characteristics of a pump-turbine and a booster pump with non-dynamic models need given pump characteristics as input. Suter characteristics curves are a way to implement given pump characteristics where four quantities are involved; the head H , the flow rate Q , the torque T and the rotational speed n . Two of the quantities can be considered independent, meaning that they can be calculated from the other two. Describing transient flow through a pump using steady-state characteristics, forces the assumption that the characteristics hold for a transient sit-

uation. Furthermore, an assumption that the homologous pump relationships, also known as the affinity laws, are valid. Dimensionless parameters are introduced for further simplicity[11].

$$h = \frac{H}{H_R} \quad \beta = \frac{T}{T_R} \quad v = \frac{Q}{Q_R} \quad \alpha = \frac{n}{n_R} \quad (2.26)$$

With subscript R referring to rated quantities, which appears at the best efficiency point. By combining the dimensionless characteristics and the pump affinity laws, the homologous relationships is given as[11]:

$$\frac{h}{\alpha^2} \text{ vs. } \frac{v}{\alpha} \quad \frac{h}{v^2} \text{ vs. } \frac{\alpha}{v} \quad \frac{\beta}{\alpha^2} \text{ vs. } \frac{v}{\alpha} \quad \frac{\beta}{v^2} \text{ vs. } \frac{\alpha}{v} \quad (2.27)$$

Since the dimensionless parameters will change and may go to zero during transient flow, the relationships are computationally difficult. By using Suter characteristic curves this difficulty can be avoided[11].

$$\frac{h}{\alpha^2 + v^2} \text{ vs. } \tan^{-1} \frac{v}{\alpha} \quad \frac{\beta}{\alpha^2 + v^2} \text{ vs. } \tan^{-1} \frac{v}{\alpha} \quad (2.28)$$

Where the relationships in equation 2.28 is used to represent the characteristic torque and head for the pump.

$$WH\left(\pi + \tan^{-1} \frac{v}{\alpha}\right) = \frac{h}{\alpha^2 + v^2} \quad WB\left(\pi + \tan^{-1} \frac{v}{\alpha}\right) = \frac{\beta}{\alpha^2 + v^2} \quad (2.29)$$

With the total dynamic head given as:

$$tdh = H_r h = (\alpha^2 + v^2) WH\left(\pi + \tan^{-1} \frac{v}{\alpha}\right) \quad (2.30)$$

In order to find the change in flow rate and rotational speed over a series connection of two pumps using Suter characteristic curves, three governing equations are needed. Where the first is found from the head balance equation over the two pumps[11].

$$H_{P_2} = tdh_{P_1} + tdh_{P_2} + H_{P_1} \quad (2.31)$$

Where subscripts $P1$ and $P2$ refers to pump one and two, with subscript 1 and 2 referring to before and after the pumps respectively. With $Q_{P1} = Q_{P2} = Q_R * v$, and setting $c = Q_{R_{P1}}/Q_{R_{P2}}$, plus $x = \left(\pi + \tan^{-1} \frac{v_1}{\alpha_1}\right)$, and $HPM = C_P - C_M$, the first pump governing equation is found by combining the equations 2.21 and 2.30 with equation 2.31.

$$F1 = HPM - 2BQ_R v + H_{R1} \left(\alpha_{P1}^2 + v_{P1}^2\right) WH_1(x) + HR_2 \left(\alpha_{P2}^2 + (cv_{P1})^2\right) WH_2(x) = 0 \quad (2.32)$$

The remaining governing equations are obtained by looking at the change of rotational speed for the pumps[11].

$$F2 = \left(\alpha_{P1}^2 + v_{P1}^2\right) WB_{P1}(x) + \beta_{01} - C_{311}\Delta\alpha = 0 \quad (2.33)$$

$$F3 = \left(\alpha_{P2}^2 + (cv_{P1})^2\right) WB_{P2}(x) + \beta_{02} - C_{312}\Delta\alpha = 0 \quad (2.34)$$

Where $WB(x)$ is given by equation 2.29, β_{01} and β_{02} are dimensionless values for the torque at previous time step for the reversible pump-turbine and booster pump. C_{311} and C_{312} are constants depending on the product of the weight of motor rotor and square radius of gyration and the time step length[11]. Finally, v , α_1 and α_2 are numerically calculated from the governing equations using the Newton-Rahpson method.

$$\begin{bmatrix} F_{1v} & F_{1\alpha_1} & F_{1\alpha_2} \\ F_{2v} & F_{2\alpha_1} & F_{2\alpha_2} \\ F_{3v} & F_{3\alpha_1} & F_{3\alpha_2} \end{bmatrix} \begin{bmatrix} \Delta v \\ \Delta\alpha_1 \\ \Delta\alpha_2 \end{bmatrix} = \begin{bmatrix} -F_1 \\ -F_2 \\ -F_3 \end{bmatrix} \quad (2.35)$$

By solving equation 2.35 for Δv , $\Delta\alpha_1$ and $\Delta\alpha_2$, the correct values are found when the sum of Δv , $\Delta\alpha_1$ and $\Delta\alpha_2$ is less than a set error tolerance. The iterated values are then used to set the boundaries as shown in equations 2.22 and 2.23.

2.6 Dynamic model for a reversible pump-turbine

The dynamic pump model, with flow rate positive from the lower to the upper reservoir, is represented by the momentum equation and the torque equation[8].

$$I_h \frac{dQ}{dt} = gH_t - gH \quad (2.36)$$

$$I_p \frac{d\omega}{dt} = T_G - T \quad (2.37)$$

With I_h being the hydraulic inertia of the turbine, and I_p the polar moment of inertia in the generator. When implementing the dynamic pump model using the method of characteristic, a more detailed look at the equations are needed. Starting with equation 2.36, written to fit the method of characteristics.

$$I_h \frac{Q_i - Q_{i-1}}{dt} = gH_t - (CM - CP + (B_{in} + B_{out})Q_i) \quad (2.38)$$

Where the term gH , the head over the pump given as felt by the system in previous time step, is represented by equations 2.12 and 2.13.

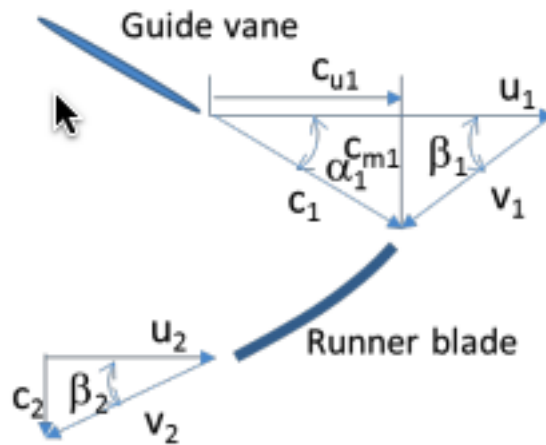


Figure 2.4: Velocity triangles at inlet and outlet of a reversible pump-turbine[8]

Starting with the Euler turbine equation leading to the hydraulic efficiency, a more detailed expression for gH_t can be found[8].

$$\eta_h \rho gQH = \rho Q(u_1 c_{u1} - u_2 c_{u2}) = \omega T \quad (2.39)$$

$$\eta_h = \frac{\omega(u_1 c_{u1} - u_2 c_{u2})}{gH} \quad (2.40)$$

With the pressure head difference between the inlet and outlet given as:

$$gH_t = u_1 c_{u1} - u_2 c_{u2} \quad (2.41)$$

Where, by looking at the inlet and outlet geometry, the $u_1 c_{u1}$ and $u_2 c_{u2}$ can be written as[8]:

$$u_1 c_{u1} = \frac{1}{2}(c_1^2 - v_1^2 + u_1^2) \quad u_2 c_{u2} = \frac{1}{2}(c_2^2 - v_2^2 + u_2^2) \quad (2.42)$$

When combining 2.41 with 2.42 the head difference is written as:

$$gH_t = \frac{1}{2}(c_1^2 - c_2^2) - \frac{1}{2}(v_1^2 - v_2^2) + s\omega \quad (2.43)$$

Where s is a geometry parameter and ω is the rotational speed.

$$s = \frac{1}{8}D_1^2 \left(1 - \frac{D_2^2}{D_1^2}\right) \quad \omega = \frac{uD}{2} \quad (2.44)$$

Another way to express the head at the design point of the turbine is[8]:

$$H = H_R \left(\frac{Q}{\kappa Q_R}\right)^2 \quad (2.45)$$

With subscript R pointing to the design point and κ representing the opening degree of the turbine. The head at design point is, similarly to equation 2.43, expressed as the difference between the inlet and outlet absolute and relative velocities[8].

$$gH_R \left(\frac{Q}{\kappa Q_R}\right)^2 = \frac{1}{2}(c_{1R}^2 - c_{2R}^2) - \frac{1}{2}(v_{1R}^2 - v_{2R}^2) + s\omega_R \quad (2.46)$$

Further combining equations 2.43 and 2.46, the head over the turbine is expressed as:

$$gH_t = gH_R \left(\frac{Q}{\kappa Q_R}\right)^2 + s(\omega - \omega_R) \quad (2.47)$$

And by linking equations 2.38 and 2.47, the version of the momentum equation used for the dynamic pump model is expressed with notations fitting the method of charac-

teristic.

$$I_h \frac{Q_i - Q_{i-1}}{dt} = gH_R \left(\frac{Q_i}{\kappa Q_R} \right)^2 s(\omega_i - \omega_R) - (CM - CP + (B_{in} + B_{out})Q_i) \quad (2.48)$$

A more detailed rewriting of the torque equation is also needed to fit the method of characteristics.

$$I_p \frac{\omega_i - \omega_{i-1}}{dt} = T_G - T \quad (2.49)$$

By looking at the Euler turbine equation, a more detailed expression for T can be found[10].

$$T = \rho Q (r_1 c_1 - r_2 c_2) \quad (2.50)$$

Where c_1 and c_2 rewritten as:

$$c_1 = \frac{Q}{A_1 \tan \alpha_1} \quad c_2 = \omega r_2 - \frac{Q}{A_2 \tan \beta_2} \quad (2.51)$$

Which, when combined with 2.50 and implemented in 2.49, provides a torque equation easily implementable in the method of characteristics.

$$I_p \frac{\omega_i - \omega_{i-1}}{dt} = T_G - (\rho Q_i (Q_i (G_1 r_1 + G_2 r_2) - \omega_i r_2^2)) \quad (2.52)$$

Where $G_1 = \frac{1}{A_1 \tan \alpha_1}$ and $G_2 = \frac{1}{A_2 \tan \beta_2}$. Leaving 2.48 and 2.52 as the two equations governing the reversible pump-turbine. With two unknowns, the new flow rate and the new rotational speed is found through iteration. The pump boundary conditions are then set by equations 2.22 and 2.23.

Modifications of governing equations

For simplicity, the momentum and torque equations are modified to where the momentum equation depends only on flow rate, while the torque equation depends on both flow rate and rotational speed. Modifying the momentum equation is done by implementing a typical pump-turbine characteristic as shown in figure 2.2 as a polynomial function to replace the term gH_t in equation 2.38. Furthermore, to simplify the

torque equation the term T_G is replaced by:

$$\frac{(r_1 - r_2)^2}{2g} \omega_i^2 \quad (2.53)$$

Leaving the torque inflicted by the generator second order dependent on rotational speed. The new expression does not have torque units, focusing mainly on the second order dependency on rotational speed for a centrifugal pump[2].

2.7 Valve

Simulating start-up conditions in a pipeline requires a valve opening gradually. Typically, for a start-up, the pumps rotate at rated rotational speed with zero flow rate in the system, leading to a high pressure at the pump-side of the valve, with a pressure drop over the valve. Modelling the flow through the valve is a function of a discharge coefficient, the area of valve opening and the pressure drop over the valve[11].

$$Q = C_d A_v \sqrt{2g\Delta H} \quad (2.54)$$

To model the valve opening a reference flow rate and reference pressure drop over the valve is needed. The reference values are found from steady-state conditions for a set opening degree[11].

$$Q_0 = C_d A_{v0} \sqrt{2gH_0} \quad (2.55)$$

By dividing equation 2.54 by equation 2.55 an equation for the flow rate through a valve with varying opening degree is found.

$$Q = Q_0 \tau \frac{\Delta H}{H_0} \quad (2.56)$$

Where τ is the dimensionless opening degree of the valve.

$$\tau = \frac{C_d A_v}{C_d A_{v0}} \quad (2.57)$$

With τ varying from 0 to 1, where 1 is the reference flow rate, and 0 is a fully closed valve. Solving equation 2.12 and equation 2.56 with respect to Q_P , with $H_P = \Delta H$ gives

an expression for the flow rate through the valve[11].

$$Q_P = -BC_v + \sqrt{(BC_v)^2 + 2C_V C_P} \quad (2.58)$$

Where $C_v = (Q_0 \tau)^2 / 2H_0$. When the flow rate is determined, the corresponding value of H_P is calculated through equation 2.12.

3. *Method*

As stated in the master thesis definition, simulating the dynamic operation of a reversible pump-turbine and a booster pump in series was the aim.

Firstly, an approach to implement the two elements in series using method of characteristic and Suter characteristic curves to represent the pump performance was investigated for possible cooperation. Secondly, a more comprehensive approach to the transient operation between the two pumps using dynamic pump models was simulated. And thirdly, the option to replace the Francis turbine in Roskrepp hydropower plant with a reversible pump-turbine and a booster pump was investigated by simulations using the dynamic pump models.

3.1 Transient model using Suter characteristic curves

For both the reversible pump-turbine and the booster pump Suter characteristic curves were implemented for a single rotational speed, which follows that the head produced from the two pumps only vary with the flow rate. The focus of this approach was to simulate how the two pumps would function together, and, therefore, a few assumptions to simplify the implementation were made. Firstly, the distance between the pumps was ignored. Secondly, the cross-sectional area of the pipes was the same throughout the pipe system. Thirdly, both inlet, outlet and machinery losses were neglected leaving frictional losses as the only loss in the system. The pump characteristics used for this approach were the characteristic curves for a reversible pump-turbine and an axial flow pump shown in figures 2.2 and 2.1 respectively. The characteristics were scaled to fit the system using affinity laws, from which the Suter characteristics curves were applied.

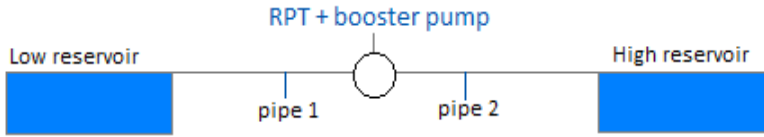


Figure 3.1: Pipe system used to implement the Suter characteristic curves

Furthermore, as shown in figure 3.1 the pipe system in which the pumps were implemented were made as non-challenging as possible; with one pipe from the lower reservoir to the pump inlet, and one pipe from the pump discharge to the higher reservoir.

Shown in algorithm 1 is the pseudocode used to implement the transient effects of pumps in series using the method of characteristics and Suter characteristic curves.

Algorithm 1 A transient system with an axial pump and a reversible pump-turbine in series using Suter characteristic curves

```

1: procedure SUTER CHARACTERISTIC CURVES
2:   Load Suter characteristic curves, including rated quantities
3:   Set initial internal conditions
4:   Use  $v, \alpha_1$  and  $\alpha_2$  to find information from the Suter curves
5:   Set initial boundary conditions
6:   for each time iteration do
7:     Initial guess at values  $v, \alpha_1$  and  $\alpha_2$ 
8:     Use  $v, \alpha_1$  and  $\alpha_2$  to find information from the Suter curves
9:     Iterate correct values for  $v, \alpha_1$  and  $\alpha_2$  using Newton-Rahpson method
10:    procedure NEWTON-RAHPSON ITERATION
11:      while  $abs(\Delta v) > \text{error tolerance}$ , do
12:        Solve the linear system of equations
13:        Update values for the flow rate and rotational speed
14:      end while
15:    end procedure
16:    Calculate internal flow values using method of characteristics
17:    Calculate boundary flow values using the corrected values of  $v, \alpha_1$  and  $\alpha_2$ 
18:  end for
19: end procedure

```

3.2 Transient model using dynamic pump models

When implementing the dynamic pump models one main difference from using Suter characteristic curves were the surge shaft between the two pumps. At first, to obtain functioning dynamic pump models a simple pipe system was used, adding a surge shaft to separate the pumps as the only difference from figure 3.1.

When implementing the pumps in Roskrepp, a model of the hydropower plant as shown in figure 3.2 was modelled. The pipe system is a simplified version of the pipelines in Roskrepp hydropower plant with a booster pump implemented at the inlet of the surge shaft. In comparison with the real pipe system, both a brook intake and a surge chamber is missing. Added simplicity comes from modelling all pipes with constant cross-sectional area.

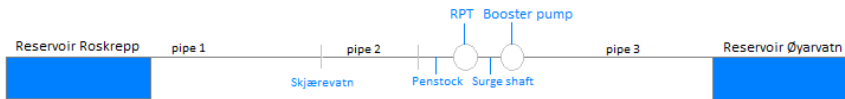


Figure 3.2: Simplified version of the Roskrepp pipe system in which the reversible pump-turbine and the booster pump were implemented

Shown in algorithm 2 is the pseudocode used when implementing transient effects over the pumps using dynamic pump models.

Algorithm 2 A transient system with an axial pump and a reversible pump-turbine in series using dynamic pump models

```

1: procedure DYNAMIC PUMP MODELS
2:   Use rated values for RPT and booster pump as initial conditions
3:   Set initial boundary conditions
4:   for each time iteration do
5:     Initial guess at values for flow rate and rotational speed
6:     Iterate values for flow rate and rotational speed
7:     procedure REVERSIBLE PUMP-TURBINE ITERATION
8:       while  $abs(\Delta q) + abs(\Delta w) > \text{error tolerance}$ , do
9:         Solve the system of equations
10:        Update values for the flow rate and rotational speed
11:      end while
12:    end procedure
13:    procedure BOOSTER PUMP ITERATION
14:      while  $abs(\Delta q) + abs(\Delta w) > \text{error tolerance}$ , do
15:        Solve the system of equations
16:        Update values for the flow rate and rotational speed
17:      end while
18:    end procedure
19:    Set boundary conditions from new values of flow rate and rotational speed
20:    Calculate internal flow values using method of characteristics
21:  end for
22: end procedure

```

4. *Results and discussions*

The result from the study of introducing a booster pump in the forefront of a reversible pump-turbine is divided into parts. Firstly, an investigation of the cooperation of an axial flow booster pump and a reversible pump-turbine in series using Suter characteristic curves. Secondly, cooperation of two elements using dynamic pump models, and thirdly the results from implementing the booster pump and a reversible pump-turbine in Roskrepp hydropower plant.

4.1 Transient model using Suter characteristic curves

Given that the implementation started from ground zero, gradual addition of elements in order to solve the thesis objective was completed. Step one being to use Suter characteristic curves to represent the pumps at one rotational speed in transient mode.

To examine how the system handles changes, a small gradual change in the upper reservoir height was introduced after 200, 500 and 850 seconds. Figure 4.1 shows that the flow stabilizes to a new steady-state rapidly after a disturbance is forced on the system boundary.

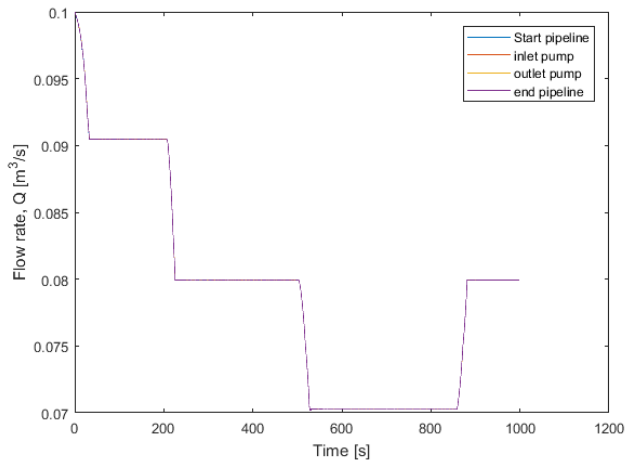


Figure 4.1: Change in flow rate over time

In figure 4.2 the modifications forced on the system are observed by looking at the change in distance between the reservoirs over time. Rapidly, the pump height delivered stabilizes and correlates with the frictional loss and the height difference between the reservoirs.

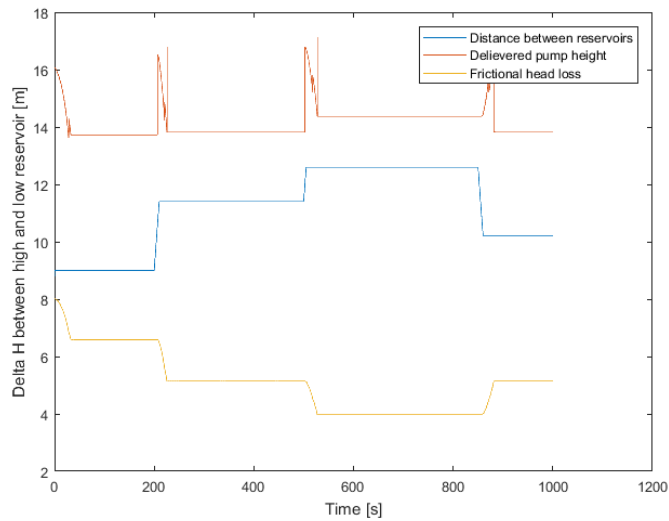


Figure 4.2: Head from the pumps, frictional loss in the system and difference in height between the reservoirs over time

As seen below in figure 4.3, when the flow reaches a steady-state there will be next to no changes in the flow rate in the pipeline. The quick stabilization provides confidence towards the cooperation, but it can also be a result of the fact that the system is only two short pipes, allowing information to move quickly from one pipe end to the other. Another important factor is the simplification to remove the distance between the pumps, allowing one single iterative process to get one shared flow rate for both pumps.

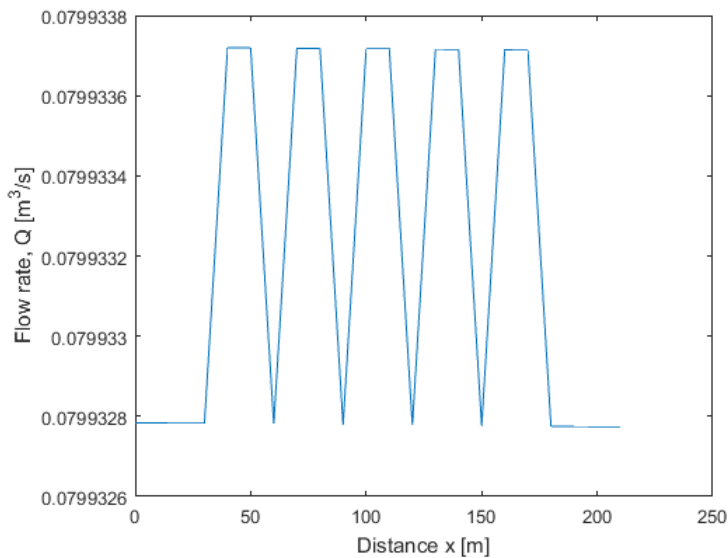


Figure 4.3: Change in flow rate through the pipes

While the simulations are providing positive results, the simplifications to the model will degrade the accuracy. When using Suter characteristic curves the pumps are modelled as one element, consisting of two pumps working in series. Therefore, a steady-state operational point comes from a combined characteristic of the two pumps, and not two separate pumps operating in series. Implemented as one element the risk of cavitation is neglected as an object of the simulation, as the pressure height at the pump-turbine inlet remains unchanged. The results still, however, justify confidence towards cooperation between an axial pump and a centrifugal pump in series, as all simulations show stable cooperation.

4.2 Cooperation using dynamic pump models

By testing the dynamic models in a similar system as for the Suter characteristic curves model, composed of only the penstock, surge shaft and pipe three as shown in figure 3.2, the cooperation of the pumps is still the main focus. The dimensions of the reversible pump-turbine used for the simulations with the dynamic model are shown in the table below.

Inlet diameter	2.68 <i>m</i>
Discharge diameter	3.2 <i>m</i>
Runner height	0.6363 <i>m</i>
Synchronous rpm	250 rpm
Rated flow	50 $m^3 s^{-1}$
Rated head	83 <i>m</i>

Table 4.1: Values for the reversible pump-turbine

A significant addition from the Suter-curve study is the introduction of the surge shaft. While the two pumps were modelled as one element using Suter characteristic curves, the implementation of the dynamic models with a surge shaft between the pumps will force the pumps to be modelled by themselves. Therefore, when modelled with dynamic models, the pumps will iterate a new rotational speed and flow rate fitting itself, not combined fitting values. Table 4.2 shows the rated values for the booster pump, which were used throughout all simulations with the dynamic model.

Rated head	20 <i>m</i>
Rated flow	50 m^3 / s
Synchronous rpm	250 <i>rpm</i>

Table 4.2: Values for the booster pump

Cooperation between the two pumps, as shown in figure 4.4, smoothly reach steady-state, and rapidly react when alterations of the reservoir heights are forced on the system. A negative aspect of the simulation results is the fluctuating period starting the simulation, where the system struggles to find a steady-state, even though the system

is fixed to begin at the rated operational point for both pumps. A probable reason for the initial fluctuating period is unbalanced governing equations, which presumably is a result of the modifications done for simplicity on the governing equations, which again results in a change in both flow rate and rotational speed. To what degree this inaccuracy affects the dynamic pump model simulations is uncertain, but how the pumps react when challenged still provide confidence in the model.

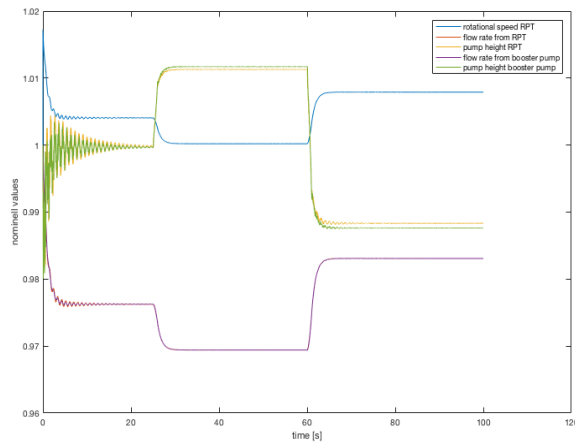


Figure 4.4: Pump height, flow rate and rotational speed changing with time

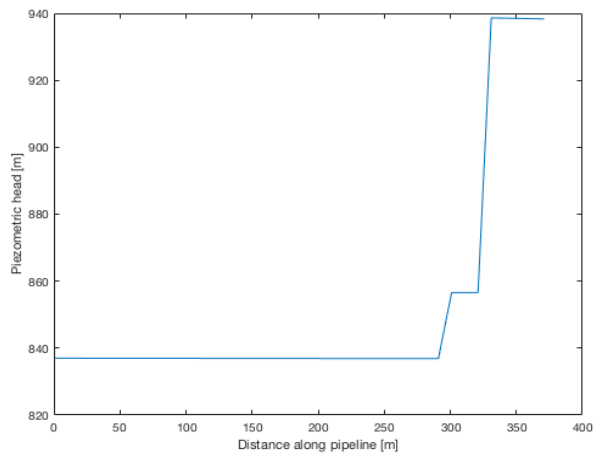


Figure 4.5: Piezometric head along the pipeline

As an indication to how introducing the booster pump will affect the parent objective of reducing the risk of cavitation in the pump-turbine, looking at figure 4.5 shows how the booster pump lifts the pressure height, leaving the pump-turbine inlet pressure to rise. Boosting the inlet pressure height increases the available $NPSH$, which decreases the risk of cavitation. For further investigation of the dynamic pump models operation, a more realistic boundary condition at the upper reservoir by introducing a periodic reservoir height is set, after an initial steady-state is reached. Figure 4.6 shows that the system reacts both rapidly and without fluctuations to the periodic change, indicating that the pump cooperation is capable of reacting to changes over time without difficulty.

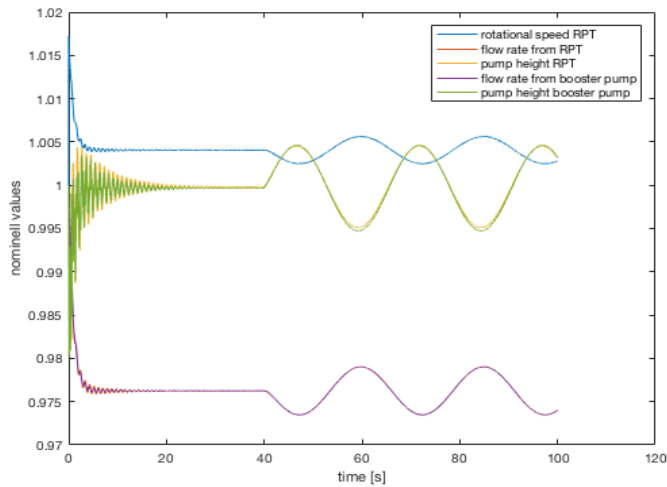


Figure 4.6: Continuous periodic change in upstream reservoir height

4.3 Dynamic pump models implemented for Roskrepp

When implementing the dynamic models at Roskrepp, the length of the pipeline is significantly increased compared to previous simulations. Comparing the results in figure 4.7 with figure 4.4 shows that the two pumps implemented in Roskrepp undoubtedly use more time to stabilize the system and find a steady-state. This delayed response is a result of information needing to travel between the pumps and the upper reser-

voir. However, when implementing the Roskrepp hydropower plant, the surge chamber was neglected for simplicity. These large long-lasting fluctuations moving from the upper reservoir to the discharge pump-turbine would be damped by introducing a surge chamber, introducing a shorter waterway from the pump to the nearest free water surface, leaving the system with less significant fluctuations[11].

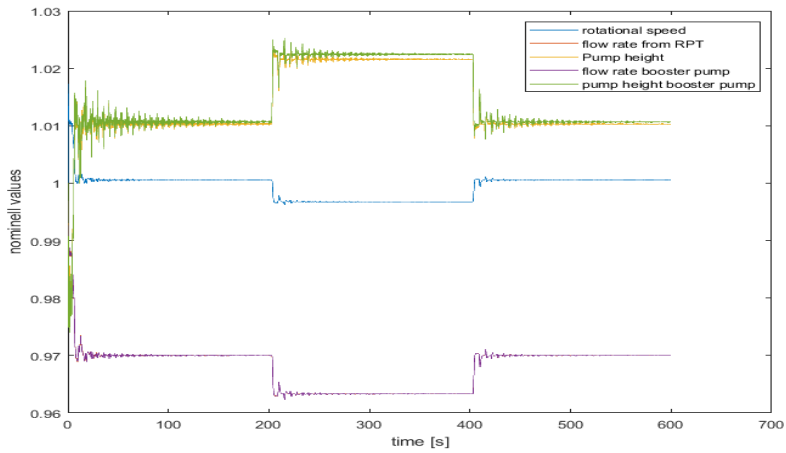


Figure 4.7: Nominal values over time

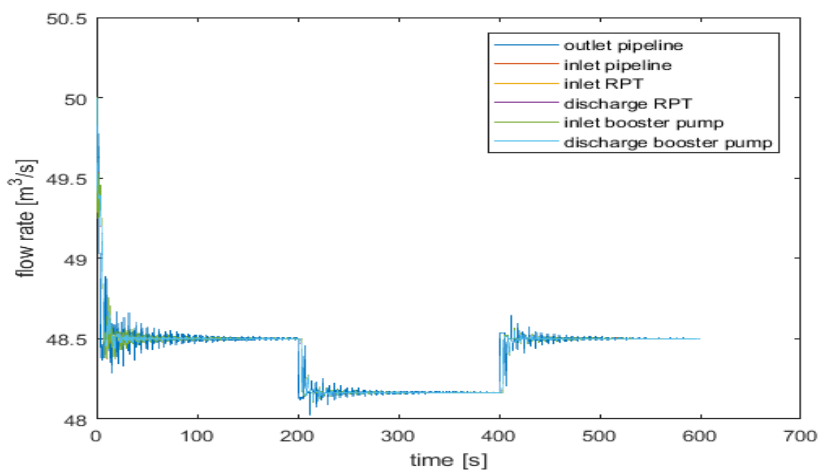


Figure 4.8: Flow rate in different points in the pipeline over time

For further investigation of the simulation results, the flow rate over time in multiple points in the pipeline are shown in figure 4.8. As a compliment to the quickness of the model; the flow rate in six different points in the pipeline follow each other closely pointing to a pump cooperation working smoothly.

4.3.1 Continuous change in boundary conditions

More realistically, investigating the cooperation of the dynamic models to a continuous change in the reservoir heights is simulated. Figure 4.9 shows how the system reacts when a periodic upper reservoir height is initialized after steady-state is reached. The system reacts, again, rapidly to the disturbances, with it being almost unaffected by the added pipe length when compared to the results from figure 4.6. The amplitude for the periodic change is only 0.5 meters and with a period of approximately 35 seconds this is not a drastic change, so for additional stability investigation, a periodic disturbance with a larger amplitude or frequency should be simulated to explore how significant or how fast disturbances the dynamic model can adapt to.

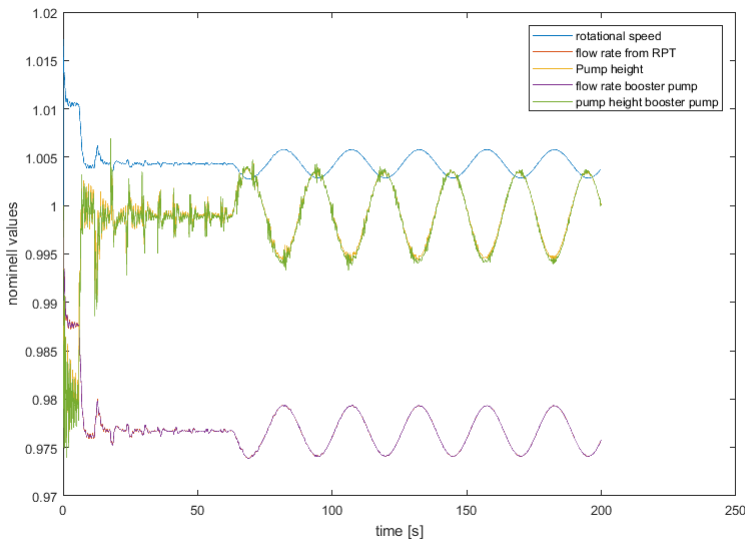


Figure 4.9: Nominal values over time with periodic change

Applying a final step towards more realistic boundary conditions was done by im-

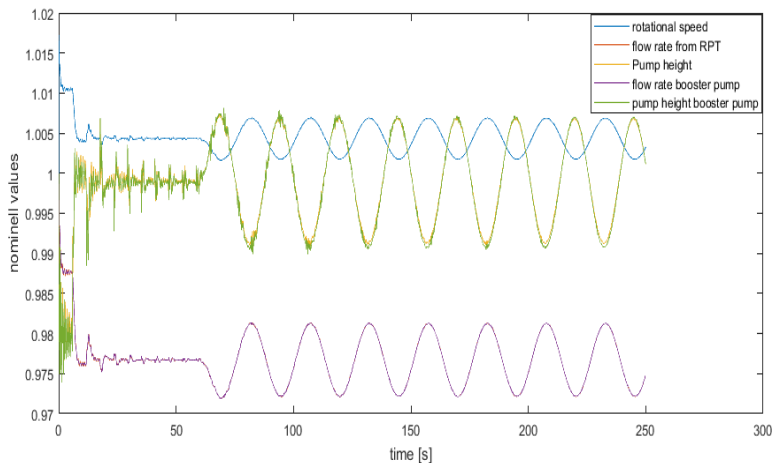


Figure 4.10: Nominal values over time when forces alterations to both reservoir heights

plementing forced periodic changes to both reservoir heights, leaving a need for the dynamic models to adjust to changing boundary conditions both upstream and downstream. Figure 4.10 shows how the pumps, again, react to the alterations both rapidly and seemingly without any fluctuations.

4.3.2 Pump start-up in Roskrepp

The start-up operation of the two pumps was simulated by introducing a valve upstream of the reversible pump-turbine. Starting at zero flow rate, with both pumps fixed at the rated rotational speed equal to 250 rpm, the start-up was executed by increasing the valve orifice linearly with time. The start-up operation did, as seen in figure 4.11, reach a steady-state, but not without fluctuations along the way. These fluctuations are a result of multiple water hammers appearing from opening the valve, which occurs as pressure waves from a significant change in flow rate over a short time[11]. With time these fluctuations disappear, with the system reaching and operating in steady-state. Worth mentioning is the instability in the pump-turbines head-flow characteristic, as shown in figure 2.2. During the start-up, the pump-turbine instability region is, when looking at figure 4.11, unnoticeable as the flow rate smoothly increases towards steady-state over the range where the instability occurs.

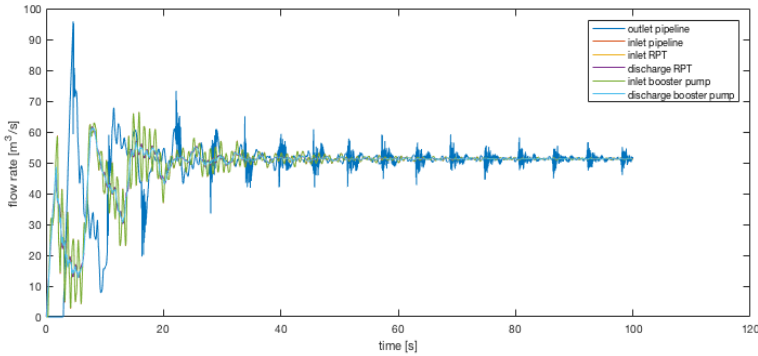


Figure 4.11: Change in flow rates during start-up

By modelling a valve that opens with 0.5 percent at each time step, the valve orifice grows linearly with time. The flow through the valve is visibly affected by the water hammer, but increases towards steady-state flow only interrupted by continuously decreasing fluctuations.

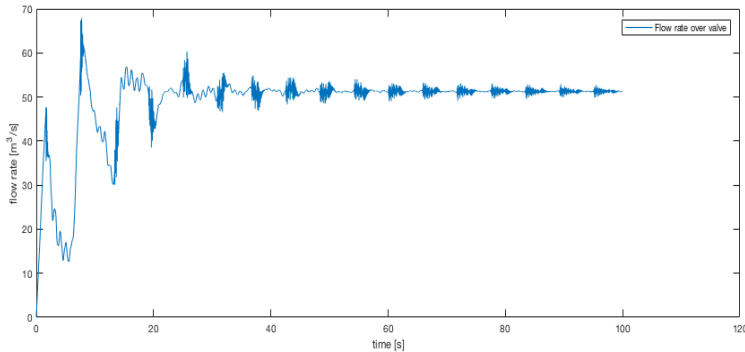


Figure 4.12: Change in flow rate over the valve during start-up

4.4 General discussions about the simulation results

Further attention to a few elements that affect the accuracy and reliability of the simulation results need to be addressed. During the process of this thesis a few significant alterations have been made.

For the reversible pump-turbine, by modifying the governing equations the accuracy of

the model undeniably decreases. Furthermore, the pump characteristic implemented in the governing equations for a high-head reversible pump-turbine, will not typically be used at a rated head as low as for Roskrepp hydropower plant. However, a typical aspect for high-head versus low-head pump-turbines is that the instability region in the pump characteristics is more substantial for high-head pump-turbines; hence the simulation results are not degraded, having implemented the more difficult option. Another aspect is the discharge diameter designed for the pump-turbine, which is larger than the existing Francis turbine inlet diameter. The increased diameter will, for the implementation in Roskrepp, either weaken the relevance of the simulation results, or require an expansion of the available runner volume, which again affects the profitability of installing a reversible pump-turbine.

Added inaccuracy comes by introducing the rim-driven thruster as an axial flow pump, with a set rotational value, varying the head delivered solely from a varying flow rate. Firstly, although an axial flow pump is similar, it is not equal to a rim-driven thruster. Secondly, the booster pump is only dependent on the flow rate, which limits the contribution of the pump, and removes a source for error in the cooperation. By modelling two pumps who are both able to adjust the rotational speed, it provides an opportunity for the booster pump to completely stop, with the reversible pump-turbine producing the entire amount of needed pressure head by altering the flow rate and rotational speed.

Worth mentioning, is that the Roskrepp hydropower plant model which was used to simulate the booster pump and reversible pump-turbine as a replacement for the Francis turbine was simplified significantly from the existing pipe system. With a constant cross-sectional surge shaft, no surge chamber and a neglected brook intake as a few of the simplifications of the hydropower plant. Adding all these elements would most definitely affect the results of the simulations, however, not necessarily in a way that degrades the overall operational results. It would instead change the response time in the system, the size of the fluctuations and therefore only the accuracy of the results achieved.

5. *Conclusion*

To conclude this master thesis, a multiple part conclusion is needed. Starting with the Suter characteristic curve transient study, looking solely on the cooperation of the two pumps, the results provide confidence towards the two pumps working together. A steady-state is quickly established, and the system accurately adjusts to forced boundary changes without large fluctuations. Although the results are providing positive results, the simplifications to the model will have to degrade the accuracy of the results. When using Suter characteristic curves, the pumps are modelled as one element, not as two separate pumps operating in series. Therefore, a steady-state operational point comes from a combined performance of the two pumps, only varying the flow rate at one rotational speed. Even with the affected accuracy of the model, the results still justify promise toward whether or not an axial pump and a centrifugal pump in series can cooperate.

The next step, implementing dynamic pump models in a simple pipeline system, also provided results where the pumps were able to cooperate in a steady fashion. While the dynamic models are more accurate than the Suter characteristic curve models, a lacking modelling of losses from both the generator and the runner will affect the accuracy of the result using dynamic models as well. Successfully reaching a steady-state and adapting to forced disturbances, both gradual and continuous periodic changes to the boundaries while iterating both the rotational speed and the flow rate, provide confidence towards the cooperation.

Replacing the Francis turbine in Roskrepp hydropower plant with a reversible pump-turbine and a booster pump resulted in similar, but somewhat slower, simulation results as to the implementation of the two pumps in a simple pipe system. Further con-

confidence as to the cooperation is attained when looking at the pump start-up simulation, which provided no difficulty in reaching full operation.

To increase the accuracy of the results a more detailed model of the Roskrepp pipe system should be implemented along with a more accurate dynamic pump model including all losses existing in the pumps and generators. An aspect to look at is the fact that the reversible pump-turbine used in the simulations had a discharge diameter larger than the Francis turbine inlet diameter, leaving a need to find a solution in which either a smaller discharge diameter or a minor adjustment to the hydropower plant layout is required. Hence, by looking at the results attained, an overall conclusion should be positive towards the idea of introducing a booster pump in the forefront of a reversible pump-turbine.

6. *Further work*

Improving the implementation of the dynamic pump models should be the primary focus. Starting with replacing the polynomials representing the pump characteristics with the terms given in equations 2.48 and 2.52. In addition, the runner and generator losses should be included in the dynamic model to increase the accuracy. Furthermore, extra attention to implementing a more detailed waterway fitting the Roskrepp hydropower plant should be modelled. Focusing on introducing a surge chamber, a brook intake, a surge shaft that varies in cross-sectional area, and smoother junctions between pipes of different sizes will all benefit the accuracy of the results.

Before replacing a Francis turbine with a reversible pump-turbine and a booster pump more specific research on both elements is needed. While, in this thesis, typical pump characteristic curves are used for both the axial flow booster pump and the reversible pump-turbine, specific models for the purpose intended should be obtained. Another element to consider for the cooperation of the two pumps is that this thesis investigates a 1D simulation, which neglects how the booster pump affects the flow that reaches the inlet of the reversible pump-turbine. Therefore, a more comprehensive study examining how the booster pump affects the fluid flow regarding rotation and turbulence for the reversible pump-turbine inlet, and how this affects the performance of the pump-turbine would be beneficial for the added accuracy of the model.

Bibliography

- [1] Qing-ming et al CAO. Prediction of loading distribution and hydrodynamic measurements for propeller blades in a rim driven thruster. *ScienceDirect Journal of Hydrodynamics*, 24(1):50–57, 2012.
- [2] Yunus A. Cengel and John M. Cimbala. *Fluid Mechanics: Fundamentals and Applications*. McGraw-Hill, 2006.
- [3] Ch Gentner et al. Numerical and experimental analysis of instability phenomena in pump turbines. *Conf. Ser.: Earth Environ. Sci.*, (15), 2012.
- [4] Anna Holm Aftret. Simulation and analysis of fcr operation of a francis turbine, 2017.
- [5] Toshiaki Kanemoto and Shin Oba. Proposition of unique pumping system with counter-rotating mechanism. *International Journal of Rotating Machinery*, 10(4):233–240, 2004.
- [6] Niroj Maharjan, Sailesh Chitrakar, and Ravi Koirala. Design of reversible pump turbine for its prospective application in nepal. 4, 07 2014.
- [7] Torbjørn K. Nielsen. Dynamic dimensioning of hydro power plants, 2015.
- [8] Torbjørn K. Nielsen. Simulation model for francis and reversible pump turbines. *International Journal of Fluid Mchinery and Systems*, 8(3), 2015.
- [9] A. J. Stepanoff. Centrifugal and axial flow pumps, 2nd edition. 1948.
- [10] Pål-Tore Storli and Torbjørn K. Nielsen. Simulation and discussion of models for hydraulic francis turbine simulations. *IFAC-PapersOnLine*, 51(2):109 – 114, 2018.

- [11] Benjamin E. Wylie and Victor L. Streeter. Fluid transients, 1983.

Appendix

6.1 Appendix A - Design reversible pump turbine

When designing a reversible pump turbine, the process is very similar to the process of designing a Francis turbine. Starting with a β_2 between 13 and 20 degrees, and u_2 between 38 and 42 m/s plus knowing the rated head and flow rate, C_{m2} , D_2 and the rotational speed can be found[6]:

$$c_{m2} = u_2 * \tan\beta_2 \quad D_2 = \sqrt{\frac{4Q}{\pi c_{m2}}} \quad n = \frac{u_2 * 60}{\pi D_2} \quad (6.1)$$

Next, the synchronous speed is found from $n = 3000/Z_p$, where Z_p is the number of pole pairs in the generator. This synchronous speed requires a set of new values[6].

$$u_{2,corrected} = \frac{n_{corrected}\pi D_2}{60} \quad \beta_2 = \tan^{-1} \frac{c_{m2}}{u_{2,corrected}} \quad (6.2)$$

Moving to the inlet, the only difference when designing a RPT versus a francis turbine comes in play. For a Francis turbine the reduced inlet peripheral velocity is 0.72, while for a reversible pump-turbine it is around 1[6].

$$u_1 = 1.05 * \sqrt{2gH} \quad D_1 = \frac{60u_1}{n\pi} \quad (6.3)$$

The outlet meridional velocity is found by assuming a 10 percent acceleration. This meridional velocity can be uses to find the inlet height[6].

$$c_{m1} = \frac{c_{m1}}{1.1} \quad B = \frac{Q}{\pi D_1 c_{m1}} \quad (6.4)$$

By using the Euler equation the reduced peripheral component of the absolute velocity can be found. C_{u1} can further be used to find the inlet blade angle.

$$c_{u1} = \frac{\eta g H}{u_1} \quad \beta_1 = \tan^{-1} \frac{c_{m1}}{u_1 - c_{u1}} \quad (6.5)$$

6.2 Appendix B - Matlab script Roskrepp waterway with RPT and booster pump - continuous periodic reservoir heights

```
clear all
close all
clc
%%ROSKREPP
```

```
i=1;
tmax=250;
```

```
%Constants
```

```
rho=1000;
g=9.81;
dx=10;
a=1200;
dt=dx/a;
f=0.04;
```

```
%system defining features
```

```
HRVhigh=929;
LDVhigh=890;
HRVlow=837;
LDVlow=820;
%Hbi=946.5;
```

```
%RPT
```

```
%Nominell values
```

```
Hr=83;%100;%83;
```

$n=250;$

$w_r=2*\pi*n/60;$

$Qr=50;$

$hpSTART=Hr;$

$q0=Qr;$

$w0=w_r;$

$q(i)=q0/Qr;$

$w(i)=w0/w_r;$

$hp(i)=hpSTART/Hr;$

$kappa(i)=1;$

$A=38.14; B_A=a/g/A;$

$P=23.4;$

$Ats=12.56; Bts=a/g/Ats;$

%RPTgeometry

$D1=3.22;$

$r1=D1/2;$

$D2=2.6814; r2=D2/2;$

$b1=0.6363;$

$beta2r=22.67;$

$a1=2*\pi*r1*b1; a2=\pi*r2^2;$

$u1r=w(i)*w_r*D1/2;$

$u2r=w(i)*w_r*D2/2;$

$u1(i)=u1r; u2(i)=u2r;$

$cm2r=u2r*\tan(beta2r*\pi/180); cmlr=cm2r/1.1;$

$cm2(i)=cm2r; cml(i)=cmlr;$

$culr=0.9/(2*1.05)*\sqrt{2*g*Hr}; cul(i)=culr;$

$beta1r=180/\pi*\atan(cmlr/(u1r-culr));$

6.2. APPENDIX B - MATLAB SCRIPT ROSKREPP WATERWAY WITH RPT AND BOOSTER PUMP - CONTIN

```

beta1(i)=beta1r;
beta2(i)=beta2r;
clr=sqrt(cmlr^2+culr^2);
cl(i)=clr;
alpha1r=180/pi*atan(cmlr/culr);
alpha1(i)=alpha1r;
psi=u2r^2/g/Hr;
xi=ulr*clr/g/Hr;
ms(i)=xi*q(i)/kappa(i)*(cos(alpha1r*pi/180)+tan(alpha1r*pi/180)...
    *sin(alpha1r*pi/180));
eta=(1-(q(i)-1)^2)*(1/hp(i)*(ms(i)-psi*w(i))*w(i));
sigma(i)=0.5*r1^2*(1-(r2/r1)^2)*w_r^2/g/Hr; %[m]

Rq(i)=D1/(2*a1*tan(beta1r*pi/180))-D2/(2*a2*tan(beta2r*pi/180)); %[
    m^-1]
G1(i)=1/(a1*tan(alpha1r*pi/180)); G2(i)=1/(a2*tan(beta2r*pi/180));
    %[m^-2]

%BOOSTER PUMP
Hb=20; hp2(i)=Hb/Hb;
Qr=50; q2(i)=Qr/Qr;
n=250;
w2r=2*pi*n/60; w2(i)=w2r;

D=sqrt(4*A/pi);

A4=38.14;
B4=a/g/A4;
L4=300;
N4=L4/dx;
R4=f*dx/(2*g*D*A4^2);

```

```

Q4=zeros(1,length(N4));
H4=zeros(1,length(N4));
for j=1:N4
    Q4(i,j)=q0;
    H4(i,j)=HRVlow-(j-1)*R4*Q4(i,j)*abs(Q4(i,j));
end
A3=38.14;
B3=a/g/A3;
L3=30;%24;
N3=L3/dx;
R3=f*dx/(2*g*D*A3^2);
Q3=zeros(1,length(N3));
H3=zeros(1,length(N3));
for j=1:N3
    Q3(i,j)=q0;
    H3(i,j)=H4(i,N4)+hp2(i)*Hb-(j-1)*R3*Q3(i,j)*abs(Q3(i,j));
end
Avalve=12.56;
Dvalve=sqrt(4*Avalve/pi);
Bvalve=a/g/Avalve;
Lvalve=10;%51;
Nvalve=Lvalve/dx;
Rvalve=f*dx/(2*g*Dvalve*Avalve^2);
Qvalve=zeros(1,length(Nvalve));
Hvalve=zeros(1,length(Nvalve));
for j=1:Nvalve
    Qvalve(i,j)=q0;
    Hvalve(i,j)=H3(i,N3)+hp(i)*Hr-(j-1)*Rvalve*Qvalve(i,j)*abs(
        Qvalve(i,j));
end

```

6.2. APPENDIX B - MATLAB SCRIPT ROSKREPP WATERWAY WITH RPT AND BOOSTER PUMP - CONTIN

```
Ats=12.56;
Dts=sqrt(4*Ats/pi);
Bts=a/g/Ats;
Lts=50;%51;
Nts=Lts/dx;
Rts=f*dx/(2*g*Dts*Ats^2);
Qts=zeros(1,length(Nts));
Hts=zeros(1,length(Nts));
for j=1:Nts
    Qts(i,j)=q0;
    Hts(i,j)=Hvalve(i,Nvalve)-(j-1)*Rts*Qts(i,j)*abs(Qts(i,j));
end

A2=38.14;
B2=a/g/A2;
L2=1310;%1311;
N2=L2/dx;
R2=f*dx/(2*g*D*A2^2);
Q2=zeros(1,length(N2));
H2=zeros(1,length(N2));
for j=1:N2
    Q2(i,j)=q0;
    H2(i,j)=Hts(i,Nts)-(j-1)*R2*Q2(i,j)*abs(Q2(i,j));
end

A1=38.14;
B1=a/g/A1;
L1=2200;%2202;
N1=L1/dx;
R1=f*dx/(2*g*D*A1^2);
Q1=zeros(1,length(N1));
```

```

H1=zeros(1,length(N1));
for j=1:N1
    Q1(i,j)=q0;
    H1(i,j)=H2(i,N2)-(j-1)*R1*Q1(i,j)*abs(Q1(i,j));
end

t(i)=0;
i=i+1;
t(i)=t(i-1)+dt;
o=dt;
p=dt;
while t(i-1)<tmax

for j=2:N4-1
CP = H4(i-1,j-1)+B4*Q4(i-1,j-1)-R4*Q4(i-1,j-1)*abs(Q4(i-1,j-1));
CM = H4(i-1,j+1)-B4*Q4(i-1,j+1)+R4*Q4(i-1,j+1)*abs(Q4(i-1,j+1));
H4(i,j) = 0.5*(CP+CM);
Q4(i,j) = 0.5*(CP-CM)/B4;
end

for j=2:N3-1
CP = H3(i-1,j-1)+B3*Q3(i-1,j-1)-R3*Q3(i-1,j-1)*abs(Q3(i-1,j-1));
CM = H3(i-1,j+1)-B3*Q3(i-1,j+1)+R3*Q3(i-1,j+1)*abs(Q3(i-1,j+1));
H3(i,j) = 0.5*(CP+CM);
Q3(i,j) = 0.5*(CP-CM)/B3;
end

for j=2:Nts-1
CP = Hts(i-1,j-1)+Bts*Qts(i-1,j-1)-Rts*Qts(i-1,j-1)*abs(Qts(i-1,j
-1));

```

6.2. APPENDIX B - MATLAB SCRIPT ROSKREPP WATERWAY WITH RPT AND BOOSTER PUMP - CONTIN

```
CM = Hts(i-1,j+1)-Bts*Qts(i-1,j+1)+Rts*Qts(i-1,j+1)*abs(Qts(i-1,j
+1));
```

```
Hts(i,j) = 0.5*(CP+CM);
```

```
Qts(i,j) = 0.5*(CP-CM)/Bts;
```

```
end
```

```
for j=2:N2-1
```

```
CP = H2(i-1,j-1)+B2*Q2(i-1,j-1)-R2*Q2(i-1,j-1)*abs(Q2(i-1,j-1));
```

```
CM = H2(i-1,j+1)-B2*Q2(i-1,j+1)+R2*Q2(i-1,j+1)*abs(Q2(i-1,j+1));
```

```
H2(i,j) = 0.5*(CP+CM);
```

```
Q2(i,j) = 0.5*(CP-CM)/B2;
```

```
end
```

```
for j=2:N1-1
```

```
CP = H1(i-1,j-1)+B1*Q1(i-1,j-1)-R1*Q1(i-1,j-1)*abs(Q1(i-1,j-1));
```

```
CM = H1(i-1,j+1)-B1*Q1(i-1,j+1)+R1*Q1(i-1,j+1)*abs(Q1(i-1,j+1));
```

```
H1(i,j) = 0.5*(CP+CM);
```

```
Q1(i,j) = 0.5*(CP-CM)/B1;
```

```
end
```

```
%BOUNDARY CONDITIONS
```

```
%between branch ts & 3
```

```
d_q=0.00001; d_w=0.00001;
```

```
%initial guess q % w
```

```
if i>2
```

```
q(i)=(q(i-1)+q(i-2))/2;
```

```
w(i)=(w(i-1)+w(i-2))/2;
```

```
kappa(i)=(kappa(i-1)+kappa(i-2))/2;
```

```
beta1(i)=(beta1(i-1)+beta1(i-2))/2;
```

```
beta2(i)=(beta2(i-1)+beta2(i-2))/2;
```

```
else
```

```
q(i)=q(i-1);
```

```
w(i)=w(i-1);
```

```
kappa(i)=kappa(i-1);
```

```
beta1(i)=beta1(i-1);
```

```
beta2(i)=beta2(i-1);
```

```
end
```

```
inertiaTexist=1;
```

```
Tm=1;
```

```
Rm=0;
```

```
Ta=6;
```

```
Tw=1;
```

```
CP=H3(i-1,N3-1)+B3*Q3(i-1,N3-1)-R3*Q3(i-1,N3-1)*abs(Q3(i-1,N3-1));
```

```
CM=Hts(i-1,2)-Bts*Qts(i-1,2)+Rts*Qts(i-1,2)*abs(Qts(i-1,2));
```

```
while (abs(d_q)+abs(d_w))>0.0000001
```

```
u2(i)=w(i)*w_r*D2/2;
```

```
u1(i)=w(i)*w_r*D1/2;
```

```
cm2(i)=u2(i)*tan(beta2(i)*pi/180);
```

```
cm1(i)=cm2(i)/1.1;
```

```
cu1(i)=g*Hr/u1(i)/0.9;
```

```
c1(i)=sqrt(cm1(i)^2+cu1(i)^2);
```

```
hp(i)=(CM-CP+(Bts+B3)*Qr*q(i))/Hr;
```

```
beta1(i)=180/pi*atan(cm1(i)/(u1(i)-cu1(i)));
```

```
beta2(i)=180/pi*atan(cm2(i)/u2(i));
```

```
alpha1(i)=180/pi*atan(cm1(i)/cu1(i));
```

```
kappa(i)=1;
```

```

G1(i)=1/(a1*tan(alpha1(i)*pi/180));
G2(i)=1/(a2*tan(beta2(i)*pi/180));

Rq(i)=D1/(2*a1*tan(beta1(i)*pi/180))...
      -D2/(2*a2*tan(beta2(i)*pi/180));
ms(i)=xi*q(i)/kappa(i)*(cos(alpha1(i)*pi/180)...
      +tan(alpha1r*pi/180)*sin(alpha1(i)*pi/180));
eta(i)=(1-(q(i)-1)^2)*(1/hp(i))*((ms(i)-psi*w(i))*w(i))
      ;
sigma(i)=0.5*r1^2*(1-(r2/r1)^2)*w_r^2/g/Hr;
rq(i)=Rq(i)*w_r*Qr/g/Hr;

Hsys=(CM-CP+(Bts+B3)*Qr*q(i));
HbyRunner=Hr*(q(i)^2/kappa(i)^2+sigma(i)*(w(i)^2-1));
Hvolumstromsaks=inertiaTexist*2*pi*r1^2*b1/a2^2*Q...
      r*(q(i)-q(i-1))/dt/g;

Tsys=(rho*Qr*q(i)*(Qr*q(i)*(G1(i)*r1+G2(i)*r2)-w_r*w(i)
      *r2^2));
Taks=Tm*w_r*(w(i)-w(i-1))/dt;
TbyGen=rho*g*Hr*Qr/(w_r);
etaG=0.95;
fun=root2dd(q(i-1),kappa(i),sigma(i),w(i-1)...
      ,Ta,Tw,dt,w_r,Qr,r1,r2,G1(i),G2(i),CM,CP,Bts,B3,Hr,
      Tm);
x0=[q(i),w(i)];
newVALUES=fsolve(fun,x0);

d_q=newVALUES(1)-q(i);
d_w=newVALUES(2)-w(i);
w(i)=w(i)+(d_w);          q(i)=q(i)+(d_q);

```

end

CP=H3(i-1,N3-1)+B3*Q3(i-1,N3-1)-R3*Q3(i-1,N3-1)*abs(Q3(i-1,N3-1));
 CM=Hts(i-1,2)-Bts*Qts(i-1,2)+Rts*Qts(i-1,2)*abs(Qts(i-1,2));

Q3(i,N3)=q(i)*Qr;
 H3(i,N3)=CP-B3*Q3(i,N3);

Qts(i,1)=Q3(i,N3);
 Hts(i,1)=CM+Bts*Qts(i,1);

%inlet downstream

if t(i-1)<60
 H4(i,1)=H4(i-1,1);
 CM=H4(i-1,2)-B4*Q4(i-1,2)+R4*Q4(i-1,2)*abs(Q4(i-1,2));
 Q4(i,1)=(H4(i,1)-CM)/B4;
 else
 H4(i,1)=H4(i-1,1)+0.5*sin(1/4*(p-dt))-0.5*sin(1/4*p);
 CM=H4(i-1,2)-B4*Q4(i-1,2)+R4*Q4(i-1,2)*abs(Q4(i-1,2));
 Q4(i,1)=(H4(i,1)-CM)/B4;
 p=p+dt;
 end

%between branch 4 & 3

%initial guess q % w

if i>2
 q2(i)=(q2(i-1)+q2(i-2))/2;
 w2(i)=(w2(i-1)+w2(i-2))/2;
 kappa(i)=1;
 else
 q2(i)=q2(i-1);

6.2. APPENDIX B - MATLAB SCRIPT ROSKREPP WATERWAY WITH RPT AND BOOSTER PUMP - CONTIN

```

w2(i)=w2(i-1);
end

d_q=0.00001; d_w=0.00001;
CP=H4(i-1,N4-1)+B4*Q4(i-1,N4-1)-R4*Q4(i-1,N4-1)*abs(Q4(i-1,N4-1));
CM=H3(i-1,2)-B3*Q3(i-1,2)+R3*Q3(i-1,2)*abs(Q3(i-1,2));
Tm2=1;
Tw2=1;
while (abs(d_q)+abs(d_w))>0.0000001

    Hsys2=(CM-CP+(B4+B3)*Qr*q2(i));
    fun2=root2d(q2(i-1),kappa(i),sigma(i),w2(i-1),...
        Ta,Tw2,dt,w_r,Qr,r1,r2,G1(i),G2(i),CM,CP,B4,B3,Hb,
        Tm2);
    x02=[q2(i)];
    newVALUES2=fsolve(fun2,x02);

    d_q=newVALUES2(1)-q2(i);
    d_w=0;%newVALUES2(2)-w2(i);
    w2(i)=w(i)+(d_w);          q2(i)=q2(i)+(d_q);

end

CP=H4(i-1,N4-1)+B4*Q4(i-1,N4-1)-R4*Q4(i-1,N4-1)*abs(Q4(i-1,N4-1));
CM=H3(i-1,2)-B3*Q3(i-1,2)+R3*Q3(i-1,2)*abs(Q3(i-1,2));

Q4(i,N4)=q2(i)*Qr;
H4(i,N4)=CP-B4*Q4(i,N4);

Q3(i,1)=Q4(i,N4);
H3(i,1)=(CM+B3*Q3(i,1));

```

$$hp2(i) = (H3(i, 1) - H4(i, N4)) / Hb;$$

%between branch ts & 2

$$CP = Hts(i-1, Nts-1) + Bts * Qts(i-1, Nts-1) - Rts * Qts(i-1, Nts-1) \dots$$

$$* abs(Qts(i-1, Nts-1));$$

$$CM = H2(i-1, 2) - B2 * Q2(i-1, 2) + R2 * Q2(i-1, 2) * abs(Q2(i-1, 2));$$

$$Qts(i, Nts) = (CP - CM) / (Bts + B3);$$

$$Q2(i, 1) = Qts(i, Nts);$$

$$Hts(i, Nts) = CM + B2 * Qts(i, Nts);$$

$$H2(i, 1) = Hts(i, Nts);$$

%between pipe branch 1 & 2

$$CP = H2(i-1, N2-1) + B2 * Q2(i-1, N2-1) - R2 * Q2(i-1, N2-1) * abs(Q2(i-1, N2-1))$$

;

$$CM = H1(i-1, 2) - B1 * Q1(i-1, 2) + R1 * Q1(i-1, 2) * abs(Q1(i-1, 2));$$

$$Q2(i, N2) = (CP - CM) / (B2 + B1);$$

$$Q1(i, 1) = Q2(i, N2);$$

$$H2(i, N2) = CM + B1 * Q2(i, N2);$$

$$H1(i, 1) = H2(i, N2);$$

%upper pipe inlet

if t(i-1) < 60

$$H1(i, N1) = H1(i-1, N1);$$

$$CP = H1(i-1, N1-1) + B1 * Q1(i-1, N1-1) - R1 * Q1(i-1, N1-1) * abs(Q1(i-1, N1-1));$$

$$Q1(i, N1) = (CP - H1(i, N1)) / B1;$$

else

$$H1(i, N1) = H1(i-1, N1) - 0.5 * \sin(1/4 * (o - dt)) + 0.5 * \sin(1/4 * o);$$

$$CP = H1(i-1, N1-1) + B1 * Q1(i-1, N1-1) - R1 * Q1(i-1, N1-1) * abs(Q1(i-1, N1-1));$$

$$Q1(i, N1) = (CP - H1(i, N1)) / B1;$$

6.2. APPENDIX B - MATLAB SCRIPT ROSKREPP WATERWAY WITH RPT AND BOOSTER PUMP - CONTIN

```
o=o+dt;
```

```
end
```

```
t(i)=t(i-1)+dt;
```

```
i=i+1;
```

```
end
```

```
x=1:dx:L1+L2+L3+Lts+L4;
```

```
H_length=zeros(1,N1+N2+Nts+N3+N4);
```

```
for l=1:length(H_length)
```

```
    if l<=N4
```

```
        H_length(1,l)=H4(end,l);
```

```
    elseif l>N4 && l<=N4+N3
```

```
        H_length(1,l)=H3(end,l-N4);
```

```
    elseif l>N4+N3 && l<=N4+N3+Nts
```

```
        H_length(1,l)=Hts(end,l-N4-N3);
```

```
    elseif l>N4+N3+Nts && l<=N4+N3+Nts+N2
```

```
        H_length(1,l)=H2(end,l-N4-N3-Nts);
```

```
    else
```

```
        H_length(1,l)=H1(end,l-N4-N3-Nts-N2);
```

```
    end
```

```
end
```

```
plot(x,H_length(1,:))
```

```
Q_length=zeros(1,N1+N2+Nts+N3+N4);
```

```
for l=1:length(Q_length)
```

```
    if l<=N4
```

```
        Q_length(1,l)=Q4(end,l);
```

```
    elseif l>N4 && l<=N4+N3
```

```
        Q_length(1,l)=Q3(end,l-N4);
```

```
    elseif l>N4+N3 && l<=N4+N3+Nts
```

```
        Q_length(1,l)=Qts(end,l-N4-N3);
```

```

elseif l>N4+N3+Nts && l<=N4+N3+Nts+N2
    Q_length(1,l)=Q2(end,l-N4-N3-Nts);
else
    Q_length(1,l)=Q1(end,l-N4-N3-Nts-N2);
end
end

Q_time=zeros(6,length(t));
for l=1:length(t)
    Q_time(1,l)=Q1(l,N1);
    Q_time(2,l)=Q4(l,1);
    Q_time(3,l)=Q3(l,N3);
    Q_time(4,l)=Qts(l,1);
    Q_time(5,l)=Q4(l,N3);
    Q_time(6,l)=Q3(l,1);
end

fricloss=zeros(1,length(t));
NPSHa=zeros(1,length(t));
NPSHr=zeros(1,length(t));
Hs=15; Ha=10.35; Hvp=0.324;
for i=1:length(t)
    for j=1:length(H4(i,:))
        fricloss(1,i)=fricloss(1,i)+R4*(Q4(i,j)*abs(Q4(i,j))...
            +Q4(i,j)*abs(Q4(i,j)));
    end
    for j=1:length(H3(i,:))
        fricloss(1,i)=fricloss(1,i)+R3*(Q3(i,j)*abs(Q3(i,j))...
            +Q3(i,j)*abs(Q3(i,j)));
    end
    for j=1:length(Hts(i,:))

```

6.2. APPENDIX B - MATLAB SCRIPT ROSKREPP WATERWAY WITH RPT AND BOOSTER PUMP - CONTIN

```

fricloss(1,i)=fricloss(1,i)+Rts*(Qts(i,j)*abs(Qts(i,j))...
    +Qts(i,j)*abs(Qts(i,j)));
end
for j=1:length(H2(i,:))
fricloss(1,i)=fricloss(1,i)+R2*(Q2(i,j)*abs(Q2(i,j))...
    +Q2(i,j)*abs(Q2(i,j)));
end
for j=1:length(H1(i,:))
fricloss(1,i)=fricloss(1,i)+R1*(Q1(i,j)*abs(Q1(i,j))...
    +Q1(i,j)*abs(Q1(i,j)));
end
NPSHr(1,i)=H3(i,N3)+Q3(i,N3)^2/A3^2/2/g-Hvp;
NPSHa(1,i)=Ha+Q3(i,N3)^2/A3^2/2/g+Hs-fricloss(1,i)-Hvp;
end

figure();
plot(t, Q_time(1,:), t, Q_time(2,:), t, Q_time(3,:), ...
    t, Q_time(4,:), t, Q_time(5,:), t, Q_time(6,:))
xlabel('time [s]');
ylabel('flow rate [m^3/s]');
legend('outlet pipeline', 'inlet pipeline', 'inlet RPT', ...
    'discharge RPT', 'inlet booster pump', 'discharge booster pump')

figure();
plot(x, Q_length(1,:));
xlabel('distance along pipeline [m]');
ylabel('flow rate [m^3/s]');

figure();
plot(t, w, t, q, t, hp, t, q2, t, hp2);

```

```
xlabel('time [s]');  
ylabel('nominell values');  
legend('rotational speed', 'flow rate from RPT', 'Pump height', ...  
       'flow rate booster pump', 'pump height booster pump')  
  
figure();  
plot(t, H3(:, N3))  
xlabel('time [s]')  
ylabel('Head inlet RPT [m]')
```

6.3 Appendix C - Matlab script function to iterate new flow rate and rotational speed RPT

function F = root2dd (q, kappa , sigma , w, Ta, Tw, dt , wr, Qr, r1 , r2 , ...

G1, G2, CM, CP, Bts , B3, Hr, Tm)

rho=1000;

g=9.81;

function E = root(x)

E(1) = -(CM-CP+(Bts+B3)*Qr*x(1))/Hr+...

(-22.28*x(1)^6+88.12*x(1)^5-129.29*x(1)^4+...

83.19*x(1)^3-20.53*x(1)^2+0.06*x(1)+1.69) -

Tw*(x(1)-q) / dt;

E(2) = (r1^2-r2^2)^2/2/g*x(2)^2 - ...

(rho*Qr*x(1)*(Qr*x(1)*(G1*r1+G2*r2)-wr*x(2)*r2^2))

- ...

Tm*(x(2)-w) / dt;

end

F=@root;

end

6.4 Appendix D - Matlab script finding RPT dimensions

```

clear all
clc
i=1;
u2(i)=36;
beta2(i)=19;
n=250;
Q=70;
H=83;
g=9.81;
eta=0.90;
i=2;
du=0.1;
dbeta=0.1;
while (du+dbeta)>0.000001
    cm2=u2(i-1)*tan(pi/180*beta2(i-1));
    D2=sqrt(4*Q/pi/cm2);
    u2(i)=n*pi*D2/60;
    beta2(i)=180/pi*atan(cm2/u2(i));
    du=abs(u2(i)-u2(i-1));
    dbeta=abs(beta2(i)-beta2(i-1));
    cm1=cm2/1.1;
    u1=1.05*sqrt(2*g*H);
    D1=u1*60/n/pi;
    cu1=H*g/eta/u1;%eta/(2*1.05)*sqrt(2*g*H);
    beta1=180/pi*atan(cm1/(u1-cu1));
    b=Q/(pi*D1*cm1);
    i=i+1;
end

```